

NUMERICAL ANALYSIS OF MECHANICAL STRESS BEHAVIOR OF ROTARY KILN OF A CEMENT PLANT

Mohammed BOUHAFS¹, Abed MEGHDIR², Yassine BELHADADJI³

¹⁾ PhD, Dept. Electromechanical, Institute of Maintenance and Industrial Safety, Univ. Oran 2, Oran, Algeria.

^{2,3)} PhD, Dept. Electromechanical, Institute of Maintenance and Industrial Safety, Univ. Oran 2, Oran, Algeria.

Abstract: Furnaces are machines that are widely used in industry, especially of cements. They are often subjected to high mechanical and thermal stress. The present work consists in modeling the mechanical behavior of a rotary kiln in stationary regime. The case studied is that of the cement factory LAFARGE Oggaz, Mascara, Algeria. This study aims is to determine the optimal operating conditions under variable mechanical loads. The two load cases considered are traction and compression of the shells. The results obtained, states of stress, deformation and displacement allow the establishment of a prediction model of the highly stressed zones and consequently to improve the parameters of design of the kiln especially in phase of dimensioning. The numerical method used is that of the finite elements as it is implemented in the ANSYS Workbench calculation code.

Key words: Rotary kiln, mechanical stress thermal stress, simulation.

1. INTRODUCTION

Rotary kilns are widely used in the cement industry as clinker production tools. They have several advantages over other types of kilns such as fixed beds; in particular being continuous kilns and the fact that production rates of flow can be high. A combustion process is necessary to convert the chemical fuel into heat capable of cooking the clinker. Insufficient heat can leave limestone particles in the clinker. Conversely, excess heat may decrease the strength of refractory bricks of the furnace, which can damage the ferrule of this one.

In this context several studies have been done, namely Brimacombe and Watkinson (1978) [1] studied the thermal behavior and the heat transfer on the wall of a rotary kiln. While Tscheng and Watkinson (1979) developed a model for calculating convective heat transfer coefficients of the wall gas. Mastrorakos et al. (1999) [2] studied the thermal behavior of a rotary kiln taking into consideration the crust layer. Nieto al (2002) [3] applied the finite element method (FEM) to determine a nonlinear analysis of a rotary kiln at the Rais HAMIDOU factory. Pazand al (2009) [4] proposed an approach for the analysis of a typical rotary kiln using the finite element method.

2. DESCRIPTION OF THE ROTARY KILN

The radial loads of the shell are transmitted to the foundations by means of tires, rollers and bearings; the

rolling stations support the kiln weight, each station comprises three main elements, each roller fixed by two bearings and tire, Figs. 1 and 2 show the general structure of a rotary kiln with the various components and principal elements that build the rotary kiln [5].

What makes rotary kilns the equipment of choice in so many processes; it is among others the fact of being

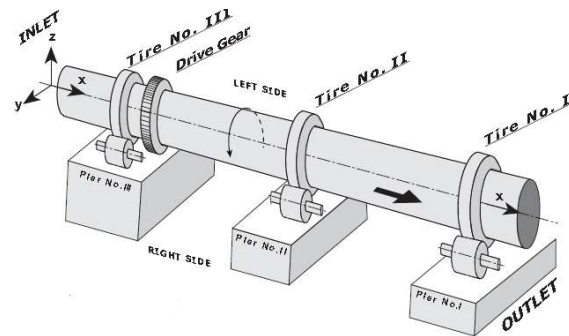


Fig. 1. Rotary kiln [5].



Fig. 2. Rollers station (tire, rollers) [7].

* Corresponding author: Institut de Maintenance et Sécurité Industrielle, Univ. Oran 2, Route de l'aéroport es Sénia, Oran Algérie,
Tel.: 21341519174; Fax: 21341519174
E-mail addresses: mohamedbouhafs@yahoo.fr (M. Bouhafs),
bjahmed1992@gmail.com (Y. Belhadadji),
meghdir.abed@yahoo.fr (A. Meghdir)

reactors of simple design. Indeed from a design point of view, a rotating kiln is an elongated cylinder inclined slightly relative to the horizontal plane and rotating around its axis. The inclination of rotary kilns is generally between 1° and 4°. A rotary kiln can quite operate with zero inclination as well. The rotational speeds usually encountered are between 0.5 rpm and 30 rpm [6].

The kiln is the centerpiece of the cement plant. Its role is to transform the prepared material into clinker by bringing it to a temperature from 1000 to 1500 °C.

The tube consists of an assembly of welded elements called shell. They are made of a quality steel sheet E 24.2 or A42 CP. The sheets with a width of about 2200 mm are rounded to the inside diameter of the kiln; the half-shells thus obtained are then welded along their two generators. The assembly of the end-to-end shell is in a staggered arrangement so as not to have an alignment of the longitudinal welds. Three types of shell can be distinguished according to their position on the axis of the kiln:

- The usual shell whose thickness varies from 22 to 36 mm
- Intermediate shell from 40 to 60 mm.
- The carrier shell or under tire from 70 to 110 mm

The torque to be transmitted requires perfect contact between the rollers and the tire. Any impact resulting from thermal deformation of the shell or settling of the foundations must be compensated by the rollers, without reducing the stability of the kiln. To reconcile these contrary requirements (optimal contact between the rolling surfaces of the rollers and the tire is isostatically supported by the shell). These kneecaps take up the supporting forces of the kiln and can follow any tire veil. This system guarantees a regular load on the generator in all load cases. To avoid wear on the rolling surfaces, the axes of rotation of the roller and the tire are always parallel during the operation of the kiln; Figure 2 shows a station that supports the weight of the kiln.

The tires, like the rollers are currently of full rectangular section, omega hollow bandages gradually disappearing. The quality of the material used is generally identical to that of the rollers. The internal diameter of the tires is slightly greater than the outer diameter of the shell with its plates to allow different expansion, because the temperature of the shell is always higher than that of the tire. Two different techniques are used for the radial positioning of the tire, depending on whether it is floating or notched [5].

3. DESCRIPTION OF THE PROBLEM

During the time of its normal operation, the kiln undergoes deformations often located in the areas near the supports. The shell releases heat by convection to the air surrounding the kiln, by conduction to other parts in contact (tire) and by radiation. In this work we study the mechanical behavior of a rotary kiln of the LAFARGE OGGAZ cement plant, we took the case of a horizontal kiln animated with a rotation movement up to 4 rpm and a weight of 700 tons, neglecting the inclination.

A numerical simulation is carried out by ANSYS Workbench to determine the stress distribution,

mechanical deformations and bending arrow. For the case studied, the kiln is considered as a set of shells and refractory bricks, and we try to study the positioning efficiency of the supports that support the kiln. The dimensions of the studied domain and the characteristics of the materials are the following ones namely a length of the kiln of 80 m, an internal diameter of 5 m, and the number of support is 3, its inclination is 4° and the angle of rollers alignment is 30°. In the context of this simulation, the shell and the brick are considered to be isotropic, linear elastic. The boundary conditions taken are as follows: a rotation speed of 4 rpm, an earth gravity of 9.81 m/s², the driving crown load of 20 000 N and the three supports considered as cylindrical supports. The different physical and mechanical characteristics of the shell steel E24.2 and the refractory brick of the kiln studied are summarized in Tables 1 and 2.

The study is based on an analysis of stress and strain during the application of different forces on the kiln. We considered the load according to variation of flow and crusting. Thus, we can make a comparison between tests based on the results. The charge of refractory material related to the volume of brick and its size is given as follows:

$$Cr(a) = h_{brick} * 10^{-3} * \phi_N * \pi * \rho, \quad (1)$$

with h_{brick} representing the height of the brick in mm and ρ is the density of the refractory brick which is 3 t/m³.

The crust adheres better to the dolomite and slightly less to the magnesia-chrome with silicate liaison and much less to the magnesia-chrome bricks with direct liaison and spinel.

This is explained by the fact that dolomite contains lime and impurities (silica, alumina and iron) which interact with the compounds of the clinker with establishment of connecting bridges; the crusting load is given by:

$$Cc(a) = h_{croustage} \cdot 10^{-3} \cdot (\phi_N - 2h_{brique}) \cdot \pi \cdot \rho', \quad (2)$$

where $h_{croustage}$ represents the height of the crust and is estimated at around 80 mm and ρ' is the crust density equal to 3 t/m³.

Table 1

The characteristics of shell [07]

Steel property E24.2	Value
Modulus of elasticity (N / m2)	2.100000031 10 ¹¹
Shear modulus (N / m2)	7.9 10 ¹⁰
Poisson coefficient	0.28
Density (kg / m3)	7800
Traction limit (N / m2)	420000000
Elasticity limit (N / m2)	275000000

Table 2

The characteristics of refractory brick [07]

Firebrick property	Value
Thermal conductivity (W / (m ° C))	1.629
Density (kg / m3)	3000
Young's module (GPa)	8
Thickness (mm)	200

Table 3

The applied loads on the kiln

Linear load	t/m	N
Refractory bricks	9.42	$7.4 \cdot 10^6$
Crust	3.46	$2.7 \cdot 10^6$
Matter	4.69	$3.7 \cdot 10^6$
Shell	4.00	$3.2 \cdot 10^6$
Total	21.57	$17 \cdot 10^6$

The degree of filling of a kiln is the ratio between the section occupied by the material and the section of the kiln. The generally accepted values vary between 5 and 17% independently of the diameter of the kiln. It is evident that a kiln is all the more profitable as its degree of charge is close to 17%; the filling rate of the kiln is expressed by the value 0.14.

$$Cm(a) = 0.14 \cdot [\phi_N - 2 \cdot (h_{brique} + h_{croustage})]^2 \cdot \rho'' \quad (3)$$

with ρ'' which represents the clinker density = 1.7 t/m³.

The thickness of the shell being unknown, the linear load of the shell can be estimated for the purposes of calculation:

$$Cv(a) = \phi_N^2 \cdot 6.5 \cdot 10^{-3} \cdot \pi \cdot \rho''' \quad (4)$$

where ρ''' which represents the density of steel equal to 7.85 t/m³

Thus the total linear load of the kiln is the sum of the different loads:

$$Ct = Cr(a) + Cc(a) + Cm(a) + Cv(a) \quad (5)$$

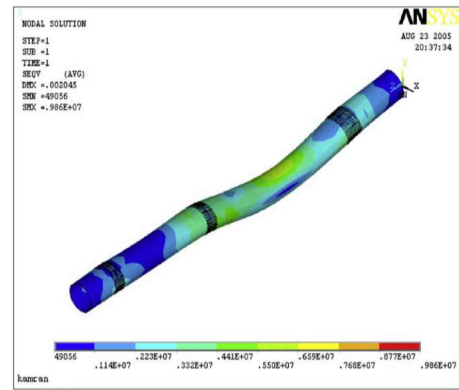
We propose to determine the different loads in the kiln (Table 3) as well as the production of cement for a kiln of 7000 t/day. The total linear charge is therefore the sum of the charges given by the equation (5).

4. COMPARISON

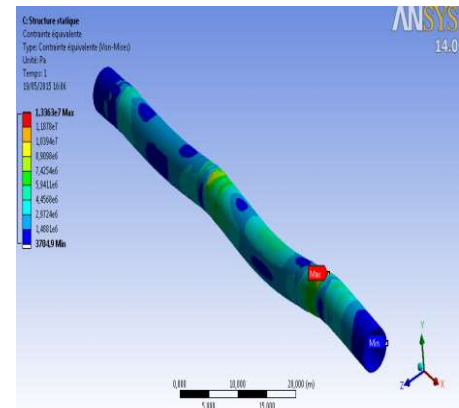
We validated our results with those of K. PAZAND [04] which are represented in Fig. 3,a. We note that the results of our simulation are very concordant with his results.

Figure 3,b (our case study) shows the Von-Mises equivalent stress distribution on the outer surface of the kiln shell. It can be seen that the Von-Mises stress varies from 3708 Pa up to 13.41 MPa, its maximum value is positioned at the support 1. We note that the distribution of stresses is greater in the first zone situated between the supports 1 and 2, while the section between the supports 2 and 3 is relatively less solicited. However at the upstream and downstream zones the stress takes the minimum value.

For the same loading conditions as those of PAZAND, the stress distribution was deduced according to the Von Mises criterion. Figure 3 shows a concordance in the distribution of stresses on the system studied namely the rotary kiln. The difference is at the maximum stress which is 13.33 MPa for our case study while that of PAZAND is 9.86 MPa. The error between the two case studies is about 25%. This is justified by the fact that the physical characteristics of the refractory brick are different, as well as the consideration of certain



a



b

Fig. 3. Representation of equivalent stress (Von Mises): a – PAZAND study; b – our study.

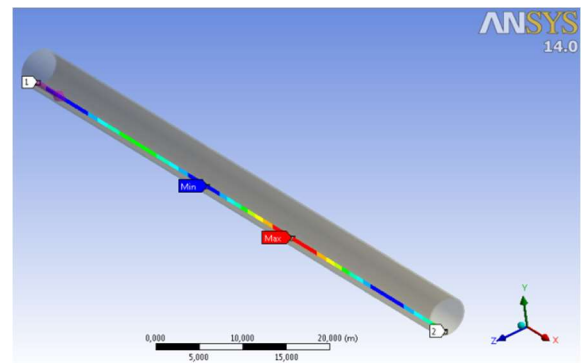


Fig. 4. Representation of the path used along the length of the kiln.

boundary conditions. So, in this case we can only compare the total behavior of the structure.

Figure 4 shows the path used to show the distribution of stresses along the rotary kiln.

Figure 5 shows the evolution of the mechanical stress along the kiln on the trajectory that we have previously represented in Fig. 4. It is noted that the stressed areas at the supports works in compression and in traction and that near the support areas there's stress concentration. We noted that downstream of the furnace the stresses concentration which is represented in Fig. 5 is less important, whereas after a distance of 5 m, the stresses increased in peak in the three stresses modes, namely maximum stress of 0.8 MPa, minimum stress of 0.5 MPa and Von Mises value of 1.5 MPa.

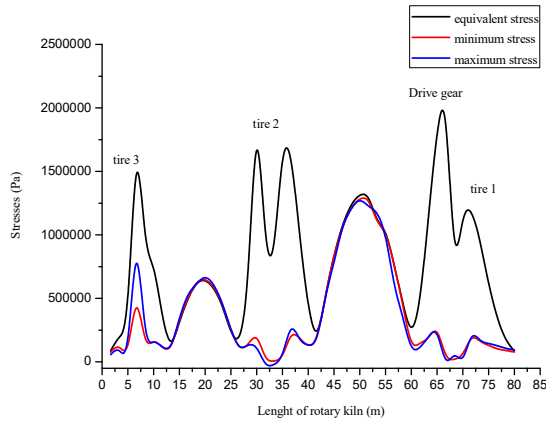


Fig. 5. The variation of the mechanical stress field.

At the level of the crown the equivalent stress takes the maximum value of 2 MPa, which is due to the weight of the crown. The maximum and minimum stresses reach their maximum of 1.3 MPa in the section between 40 m and 60 m, because of the thickness of 30 mm used in this zone of the shell.

Concerning the main maximum stresses, it appears that these stresses are more important at the winding stations (the supports). Note that the maximum equivalent stress being of the order of 15 MPa according to Fig. 6. In our case, the maximum stresses at the kiln are equal to 18.87 MPa (Fig. 5), which are slightly higher values.

Figures 7 and 8 show that the elastic deformation along the kiln is very important near the supports at the bearing stations of a value of 0.004086 compared to the other zones, because the stresses concentration is very high, which is due to the Hertzian pressure and the effect of rotation, as shown in Fig. 8.

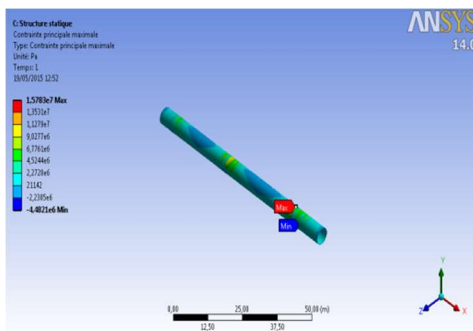


Fig. 6. Presentation of equivalent stress.

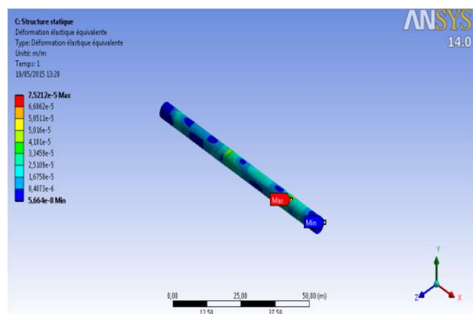


Fig. 7. Representation of the equivalent elastic strain.

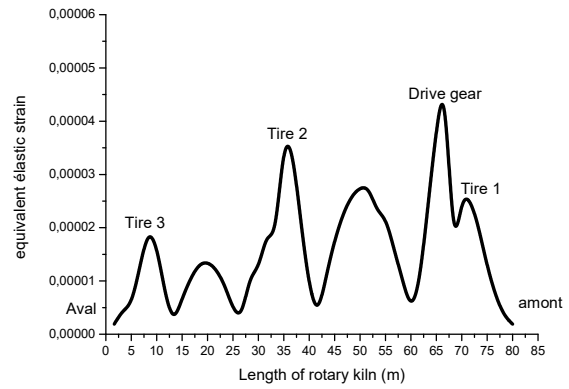


Fig. 8. Variation of the equivalent elastic strain.

Figure 8 shows that the deformation evaluated at the three stations of the bearings and the driving crown caused by the compressive force applied by the weight of the kiln. The largest strain is recorded in the direction of loading in compression and bending, i.e along $Y 5 e-5$ (the max value) at the rolling stations. We note that the most deformed areas are the thin zones (from 40 to 60 m) and at the supports (7 m support 1, 32.5 m support 2 and 69 m support 3) and the drive crown (65 m).

5. CONCLUSION

The effects of the mechanical load and the rotation velocity have a considerable effect on the behavior of the rotary kiln shells, hence the need for a maintenance program according to the properties, in order to slow down aging and reduce kiln stress (improve the fatigue behavior of the structure). This structural integrity is today a major preoccupation concerning companies operating in the cement industry in order to ensure the preservation of the environment, human safety, durability of structures and increase productivity.

The analysis of the evolution of constraints depending on the load on the kiln used to locate areas of stress concentration and thereafter propose solutions to reduce these constraints for different designs and service conditions. From our study, it was possible to deduce the following observations:

- The first is that the distribution of the stresses in the set of shells presents a danger of bending at the level of the supports. Nevertheless the maximum traction stress is lower than the elastic limit.
- Secondly, the most stressed areas are located around the bandage contact (the under bandage). In the end, it was found that the equivalent strain of the kiln has a maximum value located in the region of support that works in compression. This value, however, remains within the elastic domain.

Finally, the numerical simulation will serve us for the dimensioning, the optimization of the structural elements of wall and to avoid the damage by bursting of the structure under the pressure and the load.

REFERENCES

[1] G. Palmer and T. Howes, *Heat transfer in rotary kilns*, Technologies Pty Ltd, Brisbane, Australia, 1998.

- [2] E. Mastorakos, A. Massias, C.D. Tsakiroglou, D.A. Goussis, V.N. Burganos, and A.C. Payatakes, *CFD predictions for cement kilns including flame modelling, heat transfer and clinker chemistry*, Applied Mathematical Modelling, Vol. 23 (1999), pp. 55–76.
- [3] J.J. del Coz Diaz, F. Rodriguez Mazon, P.J. Garcia Nieto, F.J. Suarez Dominguez, *Design and finite element analysis of a wet cycle cement rotary kiln*, vol. 39 (2002), pp. 17–42.
- [4] K. Pazand, M.S. Panahi and M. Pourabdoli, *Simulating the mechanical behavior of a rotary cement kiln using artificial neural networks*, Vol. 30 (2009), pp. 3468–3473.
- [5] B. Gilbert, A. Regnault, *Fours de cimenterie, four rotatif* (Cement kilns, rotary kiln), BE 8845 Editions techniques de l'ingénieur.
- [6] B. Gilbert, Alexandre Bocan, *Fours de cimenterie, atelier de cuisson de clinker*, BE 8844 Editions techniques de l'ingénieur.
- [7] Manul FLSMidth "LAFARGE OGGAZ".
- [8] K. Peray, *The Rotary Cement Kiln, Second Edition*, Edward Arnold.
- [9] A.A. Boateng, *Rotary Kilns Transport Phenomena and Transport Processes*, Second Edition, 2015.